THE USE OF CENTRIFUGAL FIELDS IN ELECTROCHEMICAL ENERGY CONVERSION

Brian Worth
European Commission
Joint Research Centre, Ispra Site, 21020 (Varese), Italy

Intense centrifugal fields can be exploited to increase the electrochemical reaction rates in energy conversion devices such as batteries and fuel cells to improve their overall performance characteristics. This paper describes how 'spin-enhanced natural circulation', created under high centrifugal acceleration, can be used as a means for promoting an increase in mass transfer and hence reaction rates in three-dimensional porous electrodes. Some relevant scaling laws and new theoretical insights will be discussed to identify the main governing parameters in the design of centrifugal electrochemical energy-conversion systems. Recent findings obtained during the development and testing of a small prototype centrifugal zinc-air battery are presented to indicate possible trends and future prospects of this approach.

Centrifugal force has long been utilised as a means for transferring mass, momentum and energy —from ancient slingshots for hurling stones, to centrifugal pumps, to the sophisticated orbital transfer manoeuvres of interplanetary space probes. In nature, as in the man-made world, centrifugal fields are ubiquitous; we take their presence for granted. It is surprising therefore that centrifugal fields have not been exploited more, beyond common tasks such as pumping, drying and separating, in electrochemistry for example. In rotating electrochemical systems, strong centrifugal and centripetal force fields can be put to excellent use for intensifying heat and mass transfer processes at both the macro- and microscales of fluid flow, whilst promoting electron and ion transport at the nanoscale where reactions takes place. Surface tension, which usually dominates capillary-driven flow processes in porous media, can be largely suppressed by sufficiently strong centrifugal force acting on the system. In two-phase (gas-liquid) systems, the hydrodynamic behaviour of bubbles under the action of 'artificial gravity' induced by rotation can be dramatically different to that seen under normal terrestrial gravity. The transient processes of heat and mass transfer, particularly when involving phase-change during electrochemical reaction, can therefore be greatly enhanced by the body forces arising from applied centrifugal fields.

The application of centrifugal body forces in kinematic systems pre-dates by many centuries the more 'modern' developments of electrochemistry where its use as a means for intensifying process reactions is relatively new, especially in the field of energy conversion. One reason for this may be that chemistry is concerned generally with nanoscale processes, whereas centrifugal body forces manifest themselves as macroscale external fields. The relative strengths of these competing force fields is often dominated by short-range intermolecular or surface tension interactions where the correspondingly weaker external fields play no significant role. It is, however, the interplay between nanoscale and microscale phenomena that brings electrochemistry and hydrodynamics together in a synergistic way to offer potentially useful new ways of designing more efficient energy conversion devices.

Great efforts are today focussing on batteries and fuel cells as clean, efficient electrochemical energy converters. Progress in the field of fuel cell development has of late been rapid, since the early pioneering work of Davy (1802), Grove (1839) and others [1]. Most

NOMENCLATURE

a	mean pore radius
B	constant
c	concentration
C	ratio of buoyancy/capillary forces
C	Coulombs
d	bubble diameter
D	diffusion coefficient
E	enhancement coefficient
F	Faradays constant (~96,500 C)
g	gravitational acceleration (~9.81m/s^2)
h	pressure head
i	current density
I	total current
k	intrinsic permeability
K	hydraulic conductivity
l, L	length
M	species
n	effective porosity
N	angular speed (rpm)
p	pressure
q	flowrate per unit area (flux)
Q	total mass flow rate
r,R	radius, radial distance
t^+	transport number
U,V	velocity
x	distance from leading edge
y	distance normal to surface

Greek symbols

α	void fraction
α	concentration coefficient
β	coeff. of volumetric expansion
δ	boundary layer thickness
κ	thermal diffusivity
μ	coeff. of viscosity, micro-
θ	temperature difference
ρ	density
ν	kinematic viscosity μ/ρ
ω	angular velocity (rad/s)

Subscripts

b	bubble, bulk
c	centrifugal value
C	convection contribution
$crit$	critical value
D	diffusion contribution
g	gas phase
l	liquid phase
L	limiting value
0	atmospheric value, standard gravity
*	centrifugal enhanced value
∞	free stream value

modern-day fuel cells are however based on the ‘Bacon’ cell developed in the 1950's, designed somewhat like conventional batteries with planar electrodes but using consumable gaseous fuels and oxidants. In all these historically important developments, the basic configuration of the electrodes in practically all batteries and fuel cells has remained essentially unchanged, i.e. with stationary flat or concentric cylindrical plates mounted back-to-back and submersed in a liquid or gell-type electrolyte.

Fuel cells and batteries are charge-separation devices, built to convert chemical energy into electrical energy by electrochemical oxidation and reduction reactions, generating current at the active surfaces of the electrodes for use in an external circuit. The discharge reaction at the negative or metal electrode depends on the specific metal consumed, the electrolyte and various other factors, and is usually generalised as $M \rightarrow M^{n+} + ne$ where n is the *oxidation number* or number of electrons released. Faraday's second law states that, in order to liberate 1 mole of a substance, a whole number of moles of electrons must be supplied. Thus for a zinc electrode discharging to zinc ions in an aqueous solution,

$$Zn(s) \rightarrow Zn^{2+} + 2e \qquad E_0 = -0.76 \text{ V}$$

where $n = 2$ electrons are released and 2 moles of electrons are needed to discharge 1 mole of zinc ions in an electrolytic cell. When the metal is deliberately oxidized to produce current (electrons), as in a galvanic cell or battery, a potential difference E_0 is then generated across the electrodes.

Metal-air batteries (fuel cells) use neutral or alkaline electrolytes, to prevent hydrogen

generation. The oxygen-reduction half-cell reaction at the positive electrode during discharge is:

$$O_2 + 2H_2O + 4e = 4OH^- \qquad E_0 = +0.401 \text{ V}.$$

Two common metal oxidation half-cell reactions at the negative electrode during discharge (referred to the standard hydrogen electrode at pH = 14) relevant to the centrifugal metal-air cell are:

- Aluminium: $Al + 4OH^- \rightarrow Al(OH)_4^- + 3e$ $\qquad E_0 = -2.33$ V
- Zinc: $Zn + 2OH^- \rightarrow ZnO + H_2O + 2e$ $\qquad E_0 = -1.25$ V.

Three electrons are released per reaction when aluminium is oxidised, and its high open circuit voltage and specific energy make it a good candidate fuel for fuel cells. Zinc has an advantage, however, in that it's oxide can be electrically 'reconverted' back to pure metal (unlike aluminium), making zinc more attractive for 'rechargeable' batteries. Zinc metal also oxidizes less readily than does pure aluminium.

Irreversible losses occur during the electrochemical reaction process which reduce the available open-circuit voltage E_0 under discharge conditions. These losses are evidenced characteristically in the voltage-current "polarization curve" for the particular cell (Fig.1). Being current-dependent, these losses must be minimised by reducing the ohmic hindrance of all pathways through which the transfer of charge takes place. The electronic or ionic current transport between the charged species in solution and the active surface of the electrode is thus a classical diffusion-limited mass transfer process. Voltage reduces as the current drawn increases, eventually giving way to a sudden voltage reduction known as the "concentration over-voltage", when complete voltage breakdown occurs in the cell. Methods to increase the maximum current density at which voltage breakdown occurs ultimately depend on increasing the active area of the reaction zones where charge transfer takes place.

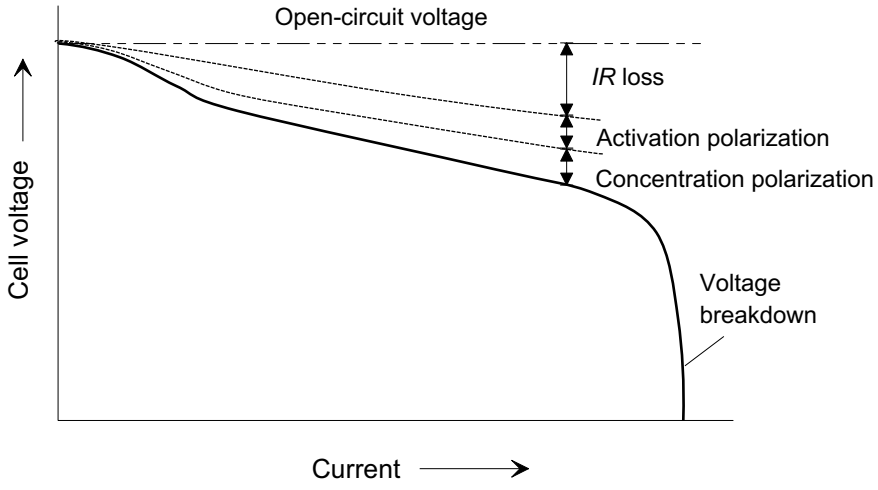

Figure 1. Typical cell polarization curve showing cell voltage as a function of discharge current

1. BACKGROUND AND PRESENT STATUS

Surprisingly little basic research has been done in the area of mass transfer with electro-chemical reaction in the presence of high-intensity centrifugal fields. Where gravity is the dominant body force, as in free convection, the classical approach in many cases may be extended, by replacing g with $\omega^2 R$ (see Table 1). Ramshaw [2-3] has described the benefits of exploiting centrifugal fields for increasing chemical and electrochemical reaction rates in a number of different devices, mainly for *process intensification* in the chemical industry. Significant increases in heat and mass transfer rates have been reported using simple rotating

systems, these increases being attributed mainly to the increased interphase buoyancy term $\Delta\rho g$ and the associated increase in local Nusselt number. Typical applications in the field of electrochemistry are in chlor-alkali production, where higher yields depend on reducing the 'overvoltage' for a given current density. Because this overvoltage is increased by the presence of gas bubbles covering the surface of the electrodes, centrifugal fields have been successfully used to 'de-gas' or 'de-aerate' the active reaction sites. Bubble detachment can be described by a type of 'centrifugal Bond number', or other related dimensionless numbers (see Table 1). This has independently raised the possibility for exploiting centrifugal fields also in power-generating devices such as fuel cells and batteries [4], using large-volume porous media for the electrodes to increase the power-density.

The high power-densities and efficiencies achieved in present-day fuel cells and batteries are undoubtedly due to improved electrode materials and catalysts. New materials such as the high porosity reticulated metal 'foams' (Fig. 2) offer optimal physical properties for the fabrication of new electrodes, particularly for the air (oxygen) electrodes of metal-air fuel cells. Heat-treated electrocatalysts of active carbon, impregnated with the so-called "transition-metal macrocyclic complexes" (porphyrin-ring structures, Fig. 3) such as cobalt tetramethoxy-phenylporphyrin (CoTMPP), exhibit a high activity and very stable long-term performance, especially at high current discharge in alkaline electrolytes [5-7]. These and other inexpensive non-precious metal catalysts show excellent electrocatalytic properties for O_2 reduction and will play an important role in the development of high power-density, large-volume 3-dimensional air-electrodes wherein current is generated throughout the bulk of the material.

Table 1. Pertinent dimensionless numbers involving gravitational body forces and their centrifugal equivalents (the hydraulic conductivity* has dimensions of a velocity *L/T*):

Dimensionless number	**Classical representation**	**Centrifugal representation**	**Significance of centrifugal effect:**
Bond No. *Bo*:	$\frac{\rho g L^2}{\sigma}$	$\frac{\rho \omega^2 R L^2}{\sigma}$	Facilitates 'dynamic detachment' of gas bubbles held by surface tension, from the electrode surfaces, so reducing 'binding' of active sites
Froude No. *Fr*:	$\frac{V}{\sqrt{gL}}$	$\frac{V}{\omega\sqrt{RL}}$	Ratio of hydrodynamic forces to gravitational or centrifugal body forces. High "*g*" implies low *Fr* hence reduced effect from waves at free-surface. When *R*~*L*, *Fr* = ratio of local velocity *V* to angular velocity ωR
Grashof No. *Gr*:	$\frac{\Delta\rho\, g L^3}{\rho \nu^2}$	$\frac{\Delta\rho\, \omega^2 R L^3}{\rho \nu^2}$	Increases buoyancy force per unit area relative to the viscous or inertial stresses, permits higher 'bubble rise velocity' and overall gas flow rate
Buoyancy parameter:	$\frac{\Delta\theta\, gL}{\theta V^2} = \frac{\Delta\rho}{\rho}\frac{1}{(Fr)^2}$	$\frac{\Delta\rho\, \omega^2 RL}{\rho V^2} = \frac{Gr_c}{(Re)^2}$	Increases free convection flow rate (higher *Gr*) with respect to local *Re*; hence increases local Nusselt No. for heat and mass transfer ($Nu = f\{Pr, Gr\}$)
Rayleigh No. *Ra*:	$\frac{\beta\, g L^3 \Delta\theta}{\nu\kappa}$	$\frac{\beta\, \omega^2 R L^3 \Delta\theta}{\nu\kappa}$	Product of *Gr* and *Pr*, ratio of thermal and momentum diffusivities which determines heat and mass transfer rates
Hydraulic conductivity* *K* or "coefficient of permeability"	$\frac{kg}{\nu}$ (k = intrinsic permeability [L^2])	$\frac{k\omega^2 R}{\nu}$	Related to Darcy's law, $\dot{q} = K\frac{\Delta h}{L} = \frac{k}{\nu}\frac{\Delta h}{L}\omega^2 R$, the hydraulic conductivity *K* expresses the ease with which fluid is transported through a porous medium. Increasing "*g*" implies higher *K* and hence higher flow rate $\dot{q}$ for a given potential head or pressure gradient $\Delta h/L$.

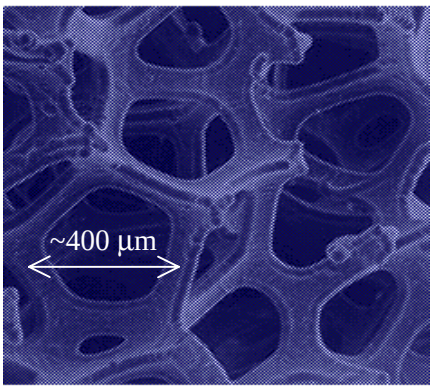

Figure 2. Magnification of a sample of reticulated nickel foam (courtesy of Recemat® International BV., Krimpen a/d Ijssel, The Netherlands); typical average pore diameter 0.4 mm, specific surface area 5600 m^2/m^3, with > 95% porosity.

But the question of how best to design practical working systems capable of using and capitalizing on these new materials is a major challenge. Mass transfer plays an essential role here, and this in turn depends on concentration gradients, local boundary layer thickness, interfacial areas for reaction and the mixing between reactants. It might be expected therefore that centrifugal body force could be used to promote strongly turbulent flow in the vicinity of an electrode to improve mass transfer. Rotation indeed appears to be an effective way for increasing mass transfer coefficients and for enhancing the performance of electrochemical devices for power generation and energy storage.

The overriding importance of hydrodynamics, and how it affects mass transfer and the ensuing electrochemical reaction rate, has long been recognised [8-9]. The deliberate application of intense centrifugal fields in order to enhance useful hydrodynamic effects however represents an important new step towards exploiting the properties of these new materials. It also marks a rather radical change in current thinking regarding the design and optimisation of fuel cells and batteries. This paper presents some new theoretical considerations and physical concepts to indicate how these ideas might be applied to the design of practical centrifugal electrochemical energy conversion devices.

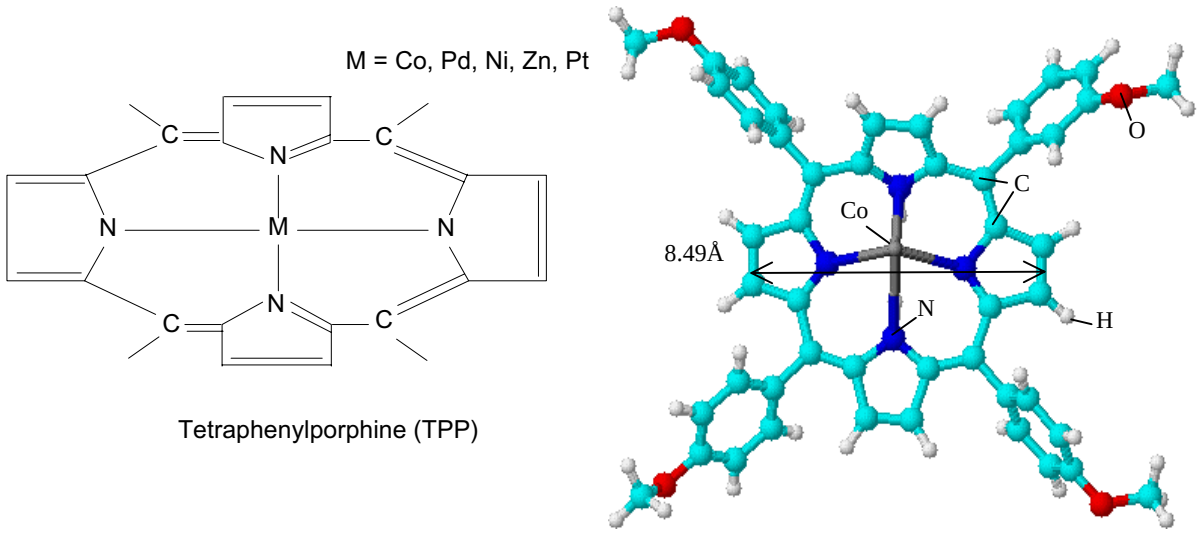

Figure 3. Bond structure of a transition metal macrocyclic compound used as the principal catalyst in an air electrode (left), with a schematic "ball&stick" model of the cobalt tetramethoxyphenylporphyrin (CoTMPP) molecule (right) showing a cobalt ion in the centre.

1.1. Current design features and limitations

Many different types of fuel cell and battery have been developed over the last 50 years (see [10-13] for many examples). Yet despite the substantial progress made in understanding and optimizing these electrochemical processes, no significant changes to basic electrode design have resulted. Indeed, the 'static' electrode configuration of modern fuel cells are practically identical in form to those in Grove's rudimentary prototypes of the 1830's, even if the materials, operating pressures, temperatures and compositions of the reactants used today have changed dramatically. It is noteworthy, therefore, that the advanced electrochemical systems now being developed, whether for generation and/or storage of electricity or for the production of industrial gases and chemicals, should still suffer the same hydro-dynamic limitations as they did in the pioneering experiments of 150 years ago.

Molecular diffusion at the electrode surface (in the "electric double-layer") ultimately governs the maximum current density and limits the achievable power output of all electrochemical energy conversion devices. The electric double-layer (Fig. 4) is, typically, less than 1nm (10Å) thick and is completely unaffected by stirring or external hydrodynamic conditions. Adjacent to this layer lies the "Nernst diffusion layer" which is typically about 0.1mm (~10^6Å) in thickness —a factor 10^5 times thicker than the electric double-layer. Charge transfer across the Nernst layer is therefore greatly influenced by local hydrodynamic flow conditions, especially near the electrode.

Despite the excellent energy-conversion efficiencies potentially attainable in theory, in practice the maximum power output of all fuel cells is limited, both thermodynamically and electrochemically, by the irreversible overpotential losses in the diffusion sub-layer. To improve power output (by making better use of the new catalysts and porous media electrodes now being developed for instance) the design of future electrochemical systems must shift away from laminar flow diffusion-limited reaction processes to forced-convection turbulent mass-transfer at the electrode surfaces. Since the electric current is determined by the rate at which ions are conveyed to an electrode surface across the diffusion sub-layer, the total current can be increased considerably by forced agitation of the solution (as noted by Levich [8]). However, it is clear that in an electrically neutral solution, the liquid in transit carries equal quantities of ions of opposite polarity and therefore the convective component in the total current flow is largely non-existent. The primary role of convection, therefore, is that it determines the *distribution* of the concentration of ions in solution, serving to decrease the thickness of the diffusion boundary layer as the free stream velocity increases.

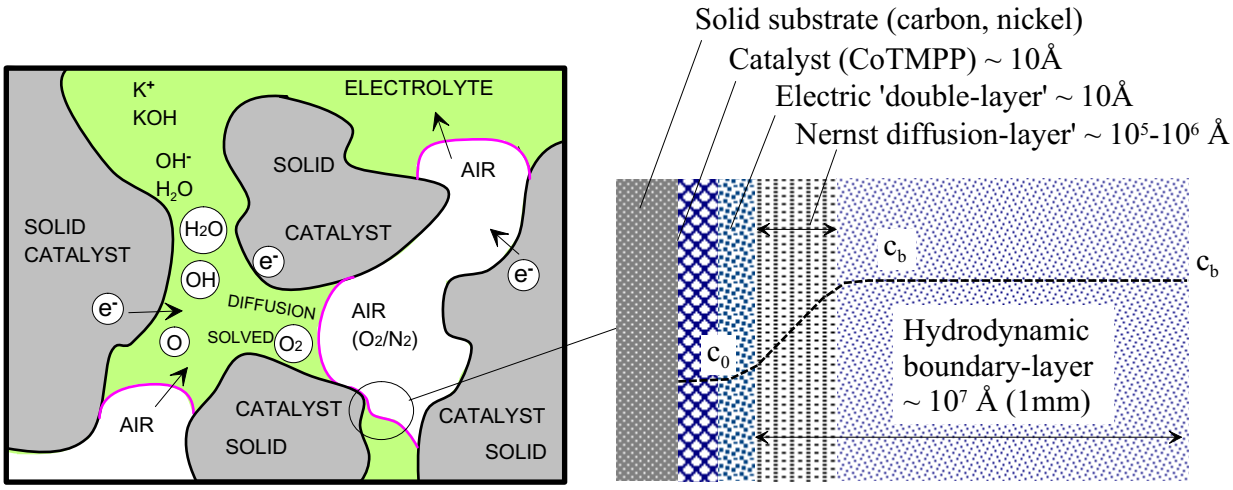

Figure 4. Schematic representation of the reaction process at the three-phase boundary of the oxygen-KOH-solid interface in an open-topology porous 3-dimensional air-electrode.

Most 'practical' fuel cell systems (e.g. those not intended for space applications) and nearly all metal-air batteries use atmospheric air as the reducing agent (oxidant) in combination with oxidisable gaseous, liquid or solid fuels. In all these systems, the 'rate-determining step' in the energy conversion process occurs at the air (oxygen) electrode. Electron transfer at the electrolyte-electrode surface is then governed by the transport of charged particles in solution at the gas-electrolyte interface. Even for electrolyte solutions that are completely saturated with reactant gas, mass transfer at the three-phase boundary surrounding a reaction site is dependent on the slow diffusion of ionic species across a liquid film adjacent to the electrode surface or between neighboring electrodes. The 'parameters' influencing the current density are therefore the species' concentrations, the diffusion coefficients, diffusion layer thickness, the active area over which the reactions take place, and the local flow conditions. A shift from laminar diffusion to turbulent hydrodynamic flow conditions can therefore have a significant influence of the prevailing mass transfer.

In non-rotating systems, diffusion is therefore across a predominantly stationary liquid film. Even if the electrolyte and reactants are pumped around the cell, quasi-static Fickian diffusion occurs across a mainly laminar viscous shear layer. This limits the mass transfer rate because the main resistance to current flow occurs across the concentration boundary layer, which is much thinner than the hydrodynamic layer and thus relatively insensitive to flow in the main stream. Independently of the flow conditions around the electrode, the diffusion sub-layer behaves is if it were in a hydrostatic quiescent liquid.

Therefore, even in pumped-systems where reactants are supplied at high pressure to the electrodes, the flow field is *over* the electrode surface; and generally no forced convection *through* the electrode occurs. Charge transfer must then take place across the quasi-stationary wetted films separating the reactant gas from the solid electrode. As a result, the fuel cell industry has developed predominantly around porous flat-plate or tubular gas-diffusion electrodes. Conventional gas-diffusion electrodes have a dry (hydrophobic) gas-side and a wetted (hydrophilic) electrolyte-side, separated by a thin wet-proof membrane. This membrane admits the flow of reactant gas from the dry side but is impermeable to the flow of electrolyte from the wetted side. Most electrodes are thus made with a layer of relatively coarse pores where the reactant gas is admitted and which remains dry, and a parallel layer of fine pores permanently filled with electrolyte. Electric current is generated only at the wetted interface between these two layers, and this process is thus essentially 2-dimensional.

An established 'rule' of electrochemistry has been that *the electrodes must not be completely flooded*. This rule arose because the wetted regions of a gas-diffusion electrode contribute little or nothing to the overall electrode current. Although much present-day research is aimed at increasing the specific surface area within the active reaction zone, this roughened active surface layer is relatively very thin in practice (~1% of the total thickness of the electrode). Flat-plate porous electrodes, despite a fractal-like appearance of their active surface layer at the molecular level, are in reality more like "2·1 dimensional" in nature and certainly not 3-dimensional.

By contrast, a true 3-dimensional porous electrode should permit a flow of reactants *everywhere* within its internal structure (Fig. 4), making contact not just across its outer surface but generating current throughout its entire volume. In practice, also this is impossible because not all of the molecular structure is accessible to flow and reactions are still highly localized. However, with extremely porous electrode structures, very large current-densities are potentially achievable if contiguous moving contact can be made with all the many interconnected conductive filaments.

The limiting current is obviously still dependent on the ohmic resistance in the solid and liquid-filled regions of the electrode, and the overpotential voltage drop across the electric double-layers, but it may nevertheless be many times greater than the current densities achievable with typical conventional flat-plate electrode technology.

Such open topology electrodes appear to violate the 'no-flooding rule', but in reality this rule only applies because of the particular two-layer electrode design, not because of any fundamental law of electrochemistry. The normal partially-flooded state of a conventional gas-diffusion electrode is therefore simply a 'stationary state' of what should be seen as a highly transient process. Thus, if air (or oxygen) is passed through the capillaries of a porous oxygen-reducing electrode, whilst simultaneously admitting a flow of liquid electrolyte, the electrochemical reaction will proceed through the forced-convection flow of reactants. The Nernst limit for mass transfer based on a flat diffusion layer is then no longer restricting and the reaction is driven instead by the hydrodynamics of the flow process itself. Moreover, the 'three-phase boundary' at the gas-electrolyte-solid interface is no longer constrained to a stationary quasi-planar boundary but will extend throughout the electrode. In continuous dynamic motion, these moving boundaries are then spatially distributed throughout the entire electrode volume, constantly creating and destroying the wetted films around a reaction site where current is generated. This dynamic process promotes a substantially higher electrochemical activity directly related to the increased Nusselt number for mass transfer, as well as permitting a much greater throughput of reactant gases than possible with stationary diffusion through a laminar boundary layer.

To date, few successful attempts have been made in designing a fuel cell system to work with pseudo 3-dimensional porous electrodes. Though the kinetics of electrode reactions in porous media are well understood (see for example Bockris & Srinivasan [9]), the main technological effort to-date seems to have focused on conventional two-layer gas-diffusion electrodes which permit only one-sided gas-phase contact but no flow-through. It seems desirable that further research is needed in this area, particularly with regard to the fabrication of porous metal foam electrodes.

An alternative approach [14] might be based on the development of a radically different type of electrochemical energy-conversion device —the ***Centrifugal Fuel Cell***. Embodiments of this approach deliberately exploit strong centrifugal fields to induce a gas-liquid flow around the cell to increase the electrochemical reaction rate, and to generate significantly more current than that needed to maintain rotation. Efficient forced-convection mass transfer at the electrode surface can be optimized by means of 'spin-enhanced natural convection' *without the need for mechanical pumps*; a big advantage when pumping highly caustic electrolyte. Another advantage of a rotating system is direct attachment to the shaft of an electric drive motor. It could also be coupled with an alternator, offering scope for a fully integrated autonomous electrochemical AC power source. A suitable device for preliminary studies is the metal-air fuel cell, and some results on the development and testing of a small prototype centrifugal zinc-air battery are presented later. A longer-term vision of the current research is the development of high-efficiency, high-power electricity generation devices in which centrifugal fields are utilized within a very compact design envelope, but this optimistic goal will be a challenge for industry to take up.

2. BASIC PRINCIPLES OF CENTRIFUGAL-FIELD ENHANCEMENT

2.1. Basic physical considerations of centrifugal fields

We consider first the origin of 'artificial gravity' created by a centrifugal field. A mass m, tethered at radial position R to a central axis and made to rotate at N revolutions per second (or $\omega = 2\pi N$ radians/second), experiences an outward centrifugal force equal to $m\omega^2 R$, balanced by an equal and opposite inward centripetal force sustained by tension in the tether. Such a mass experiences a radial force field giving it an 'apparent weight' mg, where $g = \omega^2 R$ is the centrifugal acceleration. This is the source of artificial gravity and, in accord with Einstein's 'principle of equivalence', confers identical dynamical behaviour on both gravitational and

inertial systems subjected to a steady acceleration. If the mass is displaced sideways from the spin plane, it will oscillate like a simple pendulum with periodic time $t = 2\pi\sqrt{(R/\omega^2 R)}$ under the effects of the centripetal restoring force constraining it to move in the plane of rotation. The lowest natural frequency ν is the reciprocal of the periodic time; $\nu = 1/t$ or $1/2\pi\sqrt{(R/\omega^2 R)} = N$. Thus a rotating mass displaced normal to the spin plane will oscillate *transversely* to the plane at the same frequency as its rotation speed N until the oscillations are damped. A *tangential* displacement within the plane of rotation confers no restoring force and simply adds to the rotation speed. Tethered objects in a pure centrifugal force field therefore behave as if acted upon by a steady *radial* gravitational field with local acceleration g equal to $\omega^2 R$. Particles (e.g. bubbles) in a rotating liquid also experience the same radial forces but, being subject to buoyancy, Coriolis and viscous forces, show additional dynamic and scale-related behaviour. The liquid phase thus serves to distribute the centrifugal force field throughout the continuum.

The strength of the applied centrifugal field therefore depends on the spin speed (squared) and distance from the axis of rotation. A domestic washing machine might develop an acceleration at the drum-rim of up to 400-g_0 for spin-drying purposes, when spinning at 1200 rpm. A car alternator rotates at up to 15,000 rpm, giving a centrifugal acceleration at the rotor rim of 110,000 m/s^2 or 11,300-g_o. More extreme examples are turbines and centrifugal compressors, where spin speeds of 45,000 rpm are not uncommon, giving tip accelerations in excess of 200,000-g_0. The need, and ability, to sustain high centrifugal g-loads in structural components is quite common throughout engineering, and finding sufficiently strong materials is generally not a problem. In the centrifugal fuel cell, quite low spin-speeds can often be used to good advantage, equivalent to centrifugal accelerations in the range of 100-500-g_o. Thus only moderate stresses and strains need to be tolerated in the design.

Centrifugal (and centripetal) fields are created when a 'continuum' is rotated about an axis and forces are transmitted through the medium. A mass of liquid in a closed container, undergoing 'rigid-body rotation' about an axis, transmits the centrifugal field to particles within the liquid. A bubble will accelerate and 'rise' under the influence of buoyancy caused by weight differences at a 'rise velocity' governed by the strength of the centrifugal field (plus the bubble's size, shape and viscous drag effects). As the centrifugal field varies with radial distance, its influence on the dynamic behaviour of free particles may be completely different to that of a bubble rising under terrestrial gravity in a quiescent liquid, because of hydrodynamic effects. Hydrostatic pressure, for example, varies quadratically with radius and spin-speed. Thus the density of the gas-phase, and the void-fraction and buoyancy of any two-phase mixture present in the centrifuge, are no-longer simple functions of gravity.

2.2. Main geometrical features of centrifugal power systems

The main geometrical features and principles of operation of a centrifugal system differ from those of conventional power systems. Though the electrochemistry remains essentially the same, the configuration and composition of the electrodes are designed to take advantage of the centrifugal field in order to enhance the hydrodynamic flow processes and the reaction rate.

A schematic cross-section through a centrifugal cell is shown in Fig. 5. Typically it comprises a number of flat disk- or toroidal-shaped 'fuel' and 'oxygen' electrodes, mounted in close proximity inside an electrolyte-filled inner chamber. These electrodes are stacked axially on a central shaft having an integrated air supply system, the complete assembly forming a 'rotor' which is fixed within the inner chamber and supported in bearings within an outer fixed chamber. The inner assembly can be driven, by means of an electric motor, about the spin-axis to form a *centrifuge*. Air (or oxygen) is supplied to the central shaft from where it is redistributed to various 'sparger' nozzles located at the periphery of the air-electrodes. Pairs of electrodes (anode plus cathode), immersed in a liquid electrolyte, thus form electrochemical cells in which the metal fuel anode is *oxidized* and consumed whilst oxygen (from the air or

other oxidant) is *reduced* at the cathode, producing electric current. A number of cells may be connected in series to form a battery or fuel cell with a specified voltage and power.

During operation, the inner chamber, complete with electrolyte, undergoes 'rigid-body rotation' whereby the angular velocity creates an 'artificial gravity' by virtue of the centrifugal acceleration. This increases the hydrostatic pressure within the liquid electrolyte. Electrolyte (concentrated potassium hydroxide solution) can thus circulate between the electrode chambers during rotation when a parabolic 'free surface' forms near the spin axis. The level of the electrolyte free surface is regulated by means of a 'weir-plate' of such diameter that the electrodes remain always covered, any excess liquid flowing into a small overflow reservoir for re-use. When stationary, surplus electrolyte can flow (under normal gravity) from this overflow reservoir back into the cell, ensuring that the electrodes remain covered to minimise further oxidation of the metal fuel. Air injected into, or onto, the porous oxygen-electrode (cathode) induces the *redox* reaction and this air must be supplied at a pressure somewhat higher than the hydrostatic pressure at the sparger injection point. Gaseous oxidant (air) flows from a central tube within the shaft and distributed via radial channels to an air sparger ring located at the outer periphery of the air-electrode. This is designed such that air can be supplied under pressure to the outer parts of the electrode from where it can flow uniformly inwards within various air distribution channels. Liquid electrolyte is also allowed to mix with the air to form a highly voided two-phase mixture, flowing over or through the active surfaces of the electrode. Unused air separates from the electrolyte and leaves the free surface, and discharged via internal holes to the outside of the centrifuge (it may be used also to remove unwanted heat). The atmosphere thus provides an unlimited supply of oxidant, so only fuel need be carried with the system. Figure 5 shows a schematic cross-section through the prototype centrifugal metal-air fuel cell, having a twin pair of radial disk-shaped flat-plate type of electrodes. A laboratory-scale experimental test rig has been built and tested with this configuration of electrodes.

A separate electric motor outside the cell is used to drive the centrifuge and regulate the spin-speed, through a drive gear or mounted directly on the central shaft. The motor can take its energy from the fuel cell, with 'excess' current being removed via brushes or slip-rings at the top of the shaft, or preferably via an on-axis alternator, and made available to do external work.

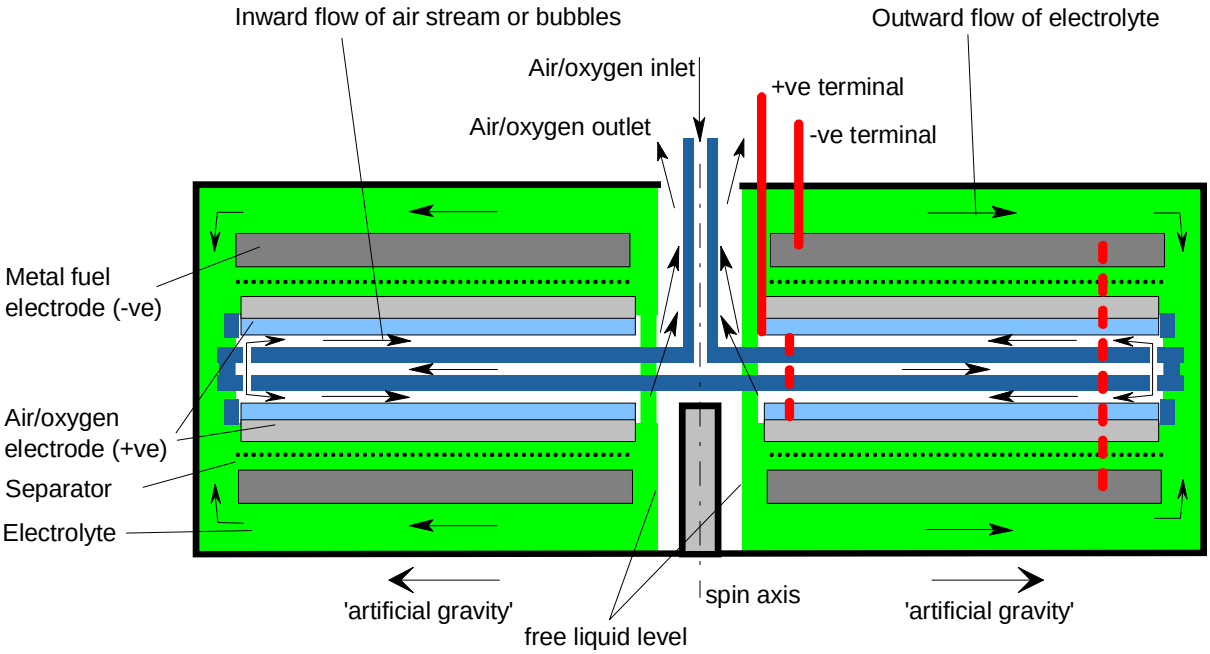

Figure 5. Cross-section through a typical centrifugal metal-air fuel cell showing radial flat-plate disk-type air and fuel electrodes.

2.3. Basic operating principles - hydrodynamic aspects

Air (or oxygen) enters the centrifuge and into the air-electrode chamber through gas spargers (Fig. 6) where very small bubbles are produced. These 'rise' towards the spin axis through the buoyancy force acting on each bubble. The buoyancy force (per unit volume) $\Delta\rho g$ is proportional to the density difference $\Delta\rho$ between the air and surrounding electrolyte, and the centrifugal acceleration $g = \omega^2 R$, and is opposed by viscous drag and any frictional resistance on the bubble, for instance from a porous medium through which it flows. When normal 1-g gravitational acceleration (~9.81 m/s^2) prevails, a bubble's 'rise velocity' in a column of static liquid is on the order of 20-30 cm/s, depending on bubble diameter, shape, viscosity and density of the surrounding liquid. Under the influence of an intensified acceleration field, this buoyancy force can propel bubbles inward at a much greater velocity, permitting a large increase in the flow rate of the reactant gases. Whether these gases be oxidants (e.g. air, oxygen) or gaseous fuels (e.g. hydrogen, hydrocarbons), the main purpose is to increase the maximum mass flow, partial pressure and density of the supplied reactants. Within the chamber (Fig. 6), the reacting mixture may be a separated disperse co-flowing gas phase within the bulk liquid electrolyte (low void fraction) or a forced flow of mainly gas with relatively little liquid phase present (high void fraction). In either case, this tends to promote efficient mass transfer at the electrode surface to an extent far greater than by static diffusion alone.

In a metal-air cell, the oxidant may be supplied to the electrode as a pressurized gas (air, oxygen), a liquid (liquid oxygen, hydrogen peroxide), or as a two-phase mixture. Oxidant injected into the electrolyte just below or inside the air-electrode chamber creates a stream of small bubbles that rise through the electrolyte-filled cavities of the porous electrode material (Figs. 4 & 6). In the extreme, this may become a column or jet of mainly air, pressurized by the hydrostatic forces on the electrolyte. On reaching the electrolyte surface near the spin-axis, unused air separates from the liquid and exits from the system. The remaining liquid electrolyte can flow back 'down', over or through the fuel electrode, towards the outer region of the centrifuge, creating a 'natural' circulating flow. A density difference then exists between the oxygen-rich fluid in the air-electrode channel ('riser'), and the gas-deficient liquid in the fuel channel ('down-comer'). Under the action of 'artificial gravity' induced by rotation, this sets up a circulating flow around the cell referred to as 'spin-enhanced natural convection'.

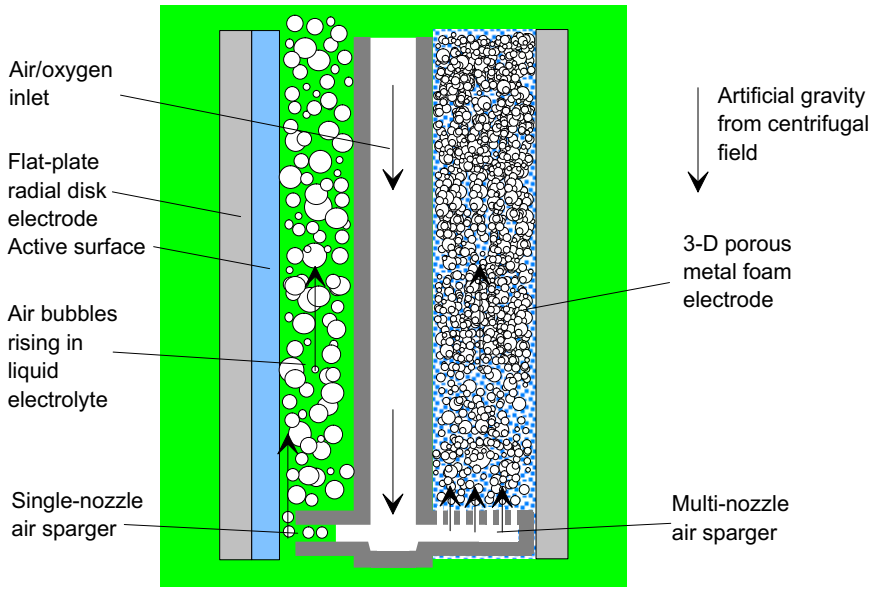

Figure 6. Typical arrangement of air sparger nozzles for a flat-plate disk air-electrode (left) and for a 3-dimensional porous metal foam air-electrode (right).

A flow of electrolyte can thus be maintained without the need for additional mechanical pumps. Considering the highly corrosive nature of concentrated electrolyte solutions on impellers, the absence of pumps in the system is a big advantage. Also, maintaining a positive flow of electrolyte around the cell serves not only to improve the hydrodynamic conditions near the electrode to increase mass transfer but also to prevent the formation and growth of *dendrite* crystals between the electrodes. Such dendrites form from precipitated electron-conducting salts and are a primary cause of short-circuits, the elimination or at least minimization of which is obviously desirable.

To enhance the reaction process in the air-electrode, porous media with a high specific surface area, such as active carbon or metal foam, should be used. However, despite the very high surface area of porous carbon (in the range 500-1200 m^2/gm), its permeability is very low at the compaction density required to maintain structural integrity, and this gives rise to high flow resistance. Thus the porosity (i.e. effective void volume divided by total bulk volume) of typical carbon electrodes is about 0.5. Carbon aerogel is also a very promising air-electrode material, with powders having extremely high surface areas (up to 2500 m^2/gm), but again low permeability presents a major problem for hydro-dynamic accessibility to the reaction sites. For very fine pores (~1 μm), a low permeability generates high capillary forces which inhibit the interpenetration of liquid. Instead of uniform dispersed flow, the injected gas may then tend to pass directly through the porous medium as localised jets in a type of 'channeling phenomenon'. It is clearly important to have a uniform distribution of air through the porous media to maximize the contact area between the oxygen of the injected air and the active catalyst sites of the electrodes. With very fine particles, capillary forces cause the wetting fluid (KOH) to adhere to the particles' surface, and air is displaced through the process of *imbibition* (see Bear [15]). Whilst the electrolyte needs to wet the electrode surface for good electrical contact, this may also prevent air bubbles in transit from penetrating the KOH film, impeding the flow of oxygen to the solid surface. In a strong centrifugal field, the wetting fluid has a greater propensity for draining from the larger pores where the acceleration field is sufficiently strong to overcome the local capillary forces. Compared to the static equilibrium case, the interpenetrating gas bubbles also divide and pass around many catalyst particles, exposing the electrodes' surface to oxygen in a dynamic manner (Fig. 4).

Understanding the dynamic behaviour of two-phase flow in a porous medium is therefore extremely important in order to optimize the design of such 3-dimensional air-electrodes, and further experimental work is needed in this area. A strong centrifugal field is used to replace gravity so as to increase the global buoyancy on a steady stream of bubbles to encourage a more uniform passage through the electrolyte-filled porous electrode than would be possible with pumped flow alone. Experiments performed under standard gravity conditions (1-*g*) indicate that, for holes less than about 4 mm in diameter, a gas bubble will not penetrate under terrestrial gravity alone. This can be inferred by comparing the buoyancy force to the capillary force for a typical bubble, where the capillary forces dominate over the viscous forces. The flow parameters of relevance are then:

- the buoyancy forces per unit area of flow cross section (across the field), which are proportional to $\left(\frac{4}{3}\pi a^3 \Delta\rho\, g\right) / \pi a^2 = \frac{4}{3}\Delta\rho\ g\, a$, where a is the 'mean pore radius' of an assumed isotropic porous medium, and
- the capillary forces per unit area of pore, in the same direction, i.e. $2\pi a\sigma / \pi a^2 = 2\sigma / a$, where σ is the gas-liquid-solid interfacial tension.

The ratio of buoyancy force to capillary force per unit area of capillary, for spherical bubbles, is then:

$$C = \frac{2}{3}\frac{a^2\, g\, \Delta\rho}{\sigma}$$

and when $C = 1$, the buoyancy and capillary forces are in balance. When $C > 1$, buoyancy dominates and a free bubble will tend to rise within the capillary tube, whereas when $C < 1$, surface tension dominates and a bubble remains trapped. For 'dirty' water, with a surface tension of say 0.1 N/m, the critical pore radius is thus about 2 mm when normal gravity (g_o = 9.81 m/s^2) is acting. Capillary tubes smaller than about 4 mm diameter thus tend to retain the water and bubble penetration does not occur.

If, on the other hand, the local gravitational field is increased, as in a centrifuge, the critical pore size is reduced and a higher acceleration greatly facilitates an easier passage of a bubble 'up' a capillary tube. The gravitational field can then be replaced by the centrifugal acceleration $\omega^2 r$ where ω is the (constant) angular velocity of rotation and R is the radial displacement from the spin-axis,

$$C = \frac{2}{3}\frac{a^2\ \Delta\rho\,\omega^2\,R}{\sigma} \approx \frac{a^2\ \rho_l\,\omega^2\,R}{\sigma} \quad \text{if } \rho_l >> \rho_g .$$

Thus for a mean pore radius of, say, 200 μm (typical of industrial metal foams), the minimum acceleration must be about 3375 m/s^2 or 345 g_o. Therefore moderately high centrifugal accelerations are necessary to induce fluid flow through a dense porous medium. Pore uniformity must be ensured to avoid 'gas channeling' although the convergent flow path on a circular disk greatly helps in this respect. Bubble impact against the filaments of the porous medium also tends to promote bubble 'break-up' and so the resulting smaller bubbles can more easily penetrate the pores of the electrode material, albeit at the expense of a higher pressure drop.

In a conventional metal-air battery, the gas-diffusion air-electrodes are generally exposed to the atmosphere. This allows a free supply of oxygen to diffuse into the porous surface of the electrode during periods of discharge. The metal fuel (e.g. zinc plate) is immersed in an ionically-conducting alkaline electrolyte (to prevent hydrogen liberation) where the metal is oxidized. Between adjacent electrodes of a cell, the ionic current can diffuse within a mainly 'static' electrolyte. The air-electrode permits absorption of oxygen on the dry-side of the air-electrode (cathode). After picking up electrons from the outer circuit, the oxygen is reduced and negatively-charged OH^- ions (*anions*) are created which diffuse through the electrolyte towards the fuel electrode (anode). At the same time, positively-charged *cations* in solution diffuse the opposite way towards the air-electrode. The free electrons thus released at the fuel electrode during the oxidation process pass around the outer circuit doing useful work. In this way, *charge-separation* occurs which is controlled mainly by the relatively slow diffusion process. Any energy released comes from a rearrangement of electrons from the higher energy-state of the reactants to a lower energy-state in the products of reaction, mainly water. In some cells, the air-electrode may also operate as a 'bi-functional' electrode, permitting oxygen liberation during charging.

Faraday's laws can be used to estimate the quantity of oxygen needed to complete the electrochemical reaction. For pure oxygen, the stoichiometric theoretical minimum O_2 flow rate is 8.28×10^{-8} kg/s per amp. With atmospheric air, the minimum air flow requirement is equivalent to about 0.4 mg/s per amp of current flowing. Because of practical difficulties in achieving a uniform distribution of oxygen throughout the electrode, more air is generally required than this theoretical minimum. The actual required air flow rate will depend not only on the current drawn but also the 'oxygen utilization factor', which must be determined from trials. Supplying more air than the minimum presents no real problem in practice, although more energy is then required for the additional compression work to overcome the hydrostatic pressure. Unused air or nitrogen from the reaction process is also useful in removing excess heat from the cell. What is important in practice is to determine the maximum amount of air that must be supplied to generate the greatest current, without displacing all the electrolyte from the active zones of the electrode or drying out the cell.

If the air-electrode comprises a porous structure with effective porosity *n*, located within the electrolyte but below the free surface, it is helpful to consider the gas-phase void fraction as a function of radius. Air will be supplied to the sparger at the 'bottom' outermost radius of the air electrode, so below this point the electrolyte is only liquid. Within a porous electrode, a two-phase mixture will 'rise' towards the central axis under the action of spin-enhanced buoyancy. The hydrostatic pressure will reduce with decreasing radius, and the specific volume of a gas bubble will increase, so for the same total mass of air flowing the void fraction will also tend to increase. Furthermore, the bubbles will 'rise' inwards into a converging flow area, so spatial flow acceleration occurs despite the reducing buoyancy at smaller radial distance. Other competing factors may also complicate the bubble rise mechanism because air is continuously absorbed into the liquid phase until it becomes saturated, so the air void fraction may tend initially to diminish with decreasing radius.

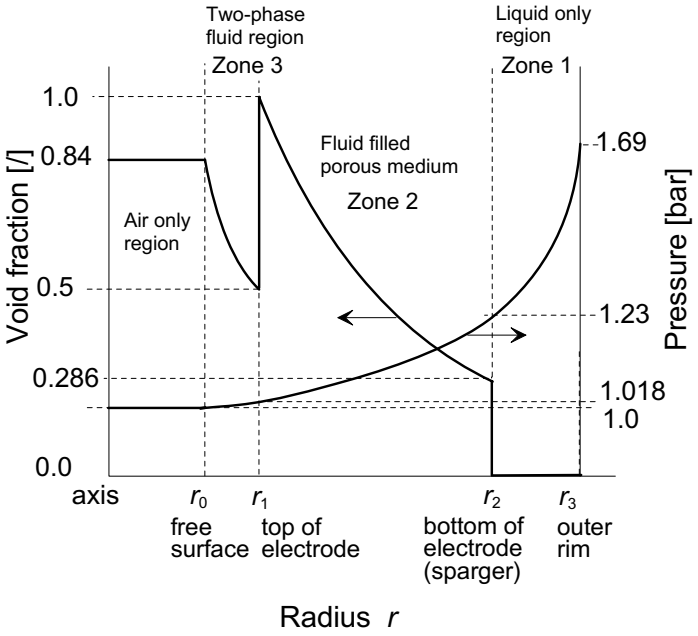

$$p(r) = p_o + \frac{1}{2}\bar{\rho}_{2\phi}\omega^2(r^2 - r_o{}^2)$$

$$\bar{\rho}_{2\phi} = \alpha_g \rho_g + (1-\alpha_g)\rho_l$$

Zone 1: $\alpha_g = 0$ (all liquid)

Zone 2: $\alpha_g(r_1) = 1$ (maximum value)

$$\alpha(r) = \frac{\alpha(r_2)r_2}{r}\left[\frac{p_1 + \frac{1}{2}\rho_l\omega^2(r_2{}^2 - r_1{}^2)}{p_1 + \frac{1}{2}\rho_l\omega^2(r^2 - r_1{}^2)}\right]$$

Zone 3: $\alpha'(r_1) = n = 0.5$ (assumed n)

$$\alpha(r) = \frac{\alpha(r_1')r_1}{r}\left[\frac{p_o + \frac{1}{2}\rho_l\omega^2(r_1{}^2 - r_0{}^2)}{p_o + \frac{1}{2}\rho_l\omega^2(r^2 - r_0{}^2)}\right]$$

Figure 7. Idealised variation of void fraction and hydrostatic pressure in the disk-shaped air-electrode chamber of a centrifugal fuel cell under two-phase flow conditions.

Whilst oxygen is absorbed at the electrode surface, gas bubbles may either coalesce or split into more numerous smaller bubbles through bubble break-up and shearing mechanisms which further helps to improve the absorption rate. Once the electrolyte becomes saturated however, the general tendency will be for the void fraction to increase as bubbles migrate inwards, and the void fraction will further increase due to the convergence of the disk-shaped flow channel. Therefore, for maximum air flow within the air-electrode, the void fraction α_g should ideally tend to 1.0 at the innermost region of the electrode (see Fig. 7).

When a 3-dimensional electrode of porosity *n* occupies the air-flow channel, the local cross-section available for flow is reduced by (1-*n*) which increases the effective volumetric gas fraction. Outside of the porous media (i.e. where *n* = 1), the void fraction again reduces but will increase further as the two-phase mixture rises to the free surface. Separation of air at the free surface then occurs, assisted by the centrifugal forces acting on the gas and liquid phases. Therefore fixing the maximum void fraction at 1.0 at the inner radius of the air-electrode allows the determination of the optimum void fraction needed at the sparger and hence the required oxidant flow rate. This procedure also allows the void fraction distribution to be calculated as a function of radius. A typical void profile is indicated in Fig. 7 along with some other parameters; for example, the pressure distribution around the cell can be determined as

well as the air mass-flow requirement and the additional compressor work needed to supply this air. A greater air flow rate could be imposed above this 'ideal limit' so long as the gas pressure at the sparger is not so high as to push the electrolyte completely out of the air electrode chamber or back into the fuel electrode region. Excessive air flow will simply displace electrolyte inwards and out of the cell, starving the electrodes of liquid, inhibiting KOH circulation and possibly preventing ion migration between the electrodes. In practice, the maximum possible air flow rate must found by experiment as the distribution and absorption of oxygen within the electrode is not known.

Input energy must be supplied to the device for acceleration and to maintain steady rotation. With typical spin-speeds of only 1000-2000 revolutions per minute, this energy 'loss' is relatively small after the initial start-up phase and can be minimized by careful design. With efficient bearings, it is estimated to be no more than a few percent of the total energy available from a centrifugal fuel cell. However, an additional 5-10% of the total available energy is also needed for the operation of ancillary components such as the compressor, and to overcome inevitable mechanical and thermal losses. The total input energy required for normal operation of a centrifugal cell is conservatively estimated to be about 10-15% of that produced in the cell. Thus the total energy conversion efficiency of such a device is expected to be about 85% or so, although these figures have not yet been confirmed in practice.

The centrifugal device therefore differs from conventional diffusion-limited 'static' devices in several important ways. Firstly, the electrochemical reaction is not necessarily confined to a planar region of the gas-diffusion electrode but is extended spatially throughout the electrode. Secondly, the 3-phase boundary is not 'static' but is in a dynamic state of continuous replenishment of the wetted films around the reaction sites. Thirdly, the mass transfer of reactants at the electrode interface is not limited by diffusion and surface tension effects but is dictated more by the prevailing turbulent hydrodynamic flow conditions near the reaction sites. Mass transfer coefficients are thereby increased as a direct consequence of the reduction in the concentration boundary-layer thickness adjacent to the surface.

2.4. Bubble dynamics in a high-*g* centrifugal field

The terminal 'rise velocity' of a bubble in a quiescent liquid is related to its Reynolds number (*Re*) and determined by its size, shape, the local buoyancy force, viscous drag and surface tension. These effects are embodied in various additional dimensionless numbers such as the Eötvös number (*Eö*) and Morton number (*Mo*) where:

$$Re = \frac{\rho_l U_b d_b}{\mu_l}, \qquad Eö = \frac{\Delta\rho\, g\, d_b^2}{\sigma} \approx \frac{\rho_l\, g\, d_b^2}{\sigma}, \qquad Mo = \frac{g\,\mu_l^4\,\Delta\rho}{\rho_l^2\,\sigma^3} \approx \frac{g\,\mu_l^4}{\rho_l\,\sigma^3}$$

and ρ_l is the liquid density, $\Delta\rho = \rho_l - \rho_g$ is the phasic density difference, σ is the interfacial tension, μ_l the liquid viscosity, d_b the equivalent bubble diameter, e.g. the diameter of a spherical bubble with the same volume, and $g = g_0$ is the acceleration due to effective gravity. In a centrifugal fuel cell, the local acceleration is increased to $g = \omega^2 r$ where ω is the angular velocity, r the radius and $g >> g_0$ (typically g = 50-500 g_o, so normal gravity can be ignored as far as bubble rise velocity is concerned). The dependence of rise velocity on *Eö* and *Mo* indicates the strong influence of gravitational acceleration on bubble motion and therefore by extension the local centrifugal acceleration in a centrifuge. Indeed, Einstein's 'principle of equivalence' holds that a bubble cannot distinguish between normal gravity-induced buoyancy and 'virtual buoyancy' arising in a centrifuge as a result of rotation.

Many empirical formulations are given for the rise velocity of a bubble in a static liquid, e.g. Levich [8], Batchelor [16], Soo [17], Butterworth & Hewitt [18], to mention few from an

extensive literature. Of relevance here however is the fact that the bubble rise velocity generally obeys a simple empirical 'power law'. Depending on the bubble's Reynolds number, $Re_b = \frac{2\rho_L u_\infty r_b}{\mu_L}$, Galileo number $\mathrm{Ga}_L = \frac{g\mu_L^4}{\rho_L \sigma^3}$ and cleanliness of the fluid, the bubble's rise velocity u_∞ is determined substantially by the local acceleration g raised to some power k. Where the local acceleration is high compared to gravitational acceleration, as for instance in a centrifuge, Butterworth & Hewitt's formula for larger bubbles where $r_b > r_{crit} = 2\left(\frac{\sigma}{g\rho_L}\right)^{0.5}$, suggests a rise velocity $u_b = 1.0(gr_b)^{0.5}$, so k has value of 0.5. When g is a function of the centrifugal acceleration, i.e. $g = \omega^2 R$, the free-stream bubble rise velocity u_b at radial position R is then directly proportional to spin speed ω. Thus for an acceleration of say 1000 m/s^2 (100-g), the critical radius r_{crit} for a spherical bubble in water is about 0.6 mm, and a bubble of 1 mm diameter would rise at about 1 m/s. Below this critical radius, viscous drag dominates and the bubble motion enters the Stokes' regime. However, the classical Stokes' law applies strictly to extremely small bubbles (where $Re_b < 2$). In a centrifuge environment, the Galileo number plays a more important role and a better formulation for bubble rise velocity has a k value of 0.25, given by:

$$u_b = 1.5\left(\frac{g\sigma}{\rho_L}\right)^{0.25} \quad \text{for } Re_b > 3Ga_L^{-0.25}.$$

Then, under an acceleration of 1000 m/s^2, an air bubble of 200 μm diameter in water has a Reynolds number of about 170 and attains a steady rise velocity of about 0.8 m/s. With g = $\omega^2 R$, the rise velocity in this case is directly proportional to $\sqrt{\omega}$ and to the fourth root of the radial displacement R. When a bubble is first released however, it accelerates very quickly to its terminal rise velocity at an initial acceleration equivalent to approximately $2\omega^2 R$ —double the maximum centrifugal acceleration.

The steady-state bubble rise velocity u_b, in an unobstructed static liquid, thus depends in large part on Re_b, on the local acceleration g, and the mean bubble radius r_b, with the overall buoyancy force being in balance with the viscous drag on the bubble. The rise velocity in the case of a centrifugal cell therefore increases in proportional to $\sqrt{\omega}$, but decreases as the bubble flows inward. However, for radial inward flow, the 'channel' also converges and the flow area thus decreases directly as R, so the void fraction tends to increase as radius decreases. This more than compensates for the tendency of bubbles to slow down as they flow inwards. As the total gas flow rate through an electrode depends on bubble rise velocity, the more oxygen passing through the electrode the higher the power-density obtainable.

A centrifugal fuel cell has typically two side-by-side chambers for each electrode, connected at the 'top' and 'bottom' to allow a circulation of electrolyte around the cell and across or through each radial disk-shaped electrode. In the narrow gap between two electrodes, electrolyte permeates to allow the passage of charged ions in solution and completes the electric circuit. Under conditions of forced flow arising from spin-enhanced convection, both the liquid and gas phases in the air-electrode channel flow inwards. In the fuel chamber, with the bulk of the gas separated from the liquid at the free surface, only pure electrolyte flows outwards, the difference in fluid density (and hence specific weight) between the two chambers setting up the pressure difference which drives the circulation.

In the case of bubbles rising through a liquid-filled porous medium, the bubbles are strongly hindered by the shearing effect of the porous matrix. Depending on the mean size of the pores relative to the bubble diameter, the interconnecting fibres of solid material act like

cutting edges and tend to slice a bubble in two. Bubble impact studies (Balasundaram *et al.* [19]) have shown that, under the influence of high acceleration and enhanced buoyancy, larger bubbles split into smaller bubbles having a much greater surface area for the same void fraction. A critical bubble size was predicted, based on simple energy considerations, above which bubble splitting tends to occur. It was found that when a bubble collided symmetrically with a vertical knife-edge, its subsequent behaviour was dictated by the sum of its buoyancy and the kinetic energy released on impact. If this exceeded the surface energy created by splitting, then breakdown would occur, otherwise bubbles would tend to bounce away from the knife-edge and stay intact. Bubble splitting is thus an advantage which occurs naturally in a dense porous medium, although capillary forces tend to retain the wetted film and this may exacerbate the oxygen transport to the catalyst.

Even for less-dense materials with a more open-structure, such as industrial packing, knitted mesh or the metal foams described previously, the average pore size may still be smaller than the mean bubble diameter at the point of gas injection, hindering a bubble's motion. In effect, a bubble must be smaller than the mean pore size to pass freely. The packing material itself must be used to split larger bubbles into smaller ones, and this mechanism clearly favours a high imposed acceleration. From the bubble impact studies of Balasundaram *et al*, the kinetic energy considerations suggest that the critical bubble diameter is reduced to about 150 μm when the maximum imposed acceleration is on the order of 370-*g*. In the absence of any packing material, the bubbles were significantly larger, typically about 1 mm in diameter. Although Balasundaram's field of application was seawater de-aeration, the effect of bubble splitting under high centrifugal acceleration in the fuel cell application considered here can be expected to increase reaction rates substantially. Materials having a porosity of 90 - 95% and a specific surface area in the range of 3000 - 6000 m^2/m^3 are considered to be most appropriate for 3-dimensional electrodes in centrifugal fuel cells. Air-electrodes made from such material should be sufficiently open to permit the unimpeded flow of air-KOH mixtures whilst giving a high contact area for reaction.

2.5. Electrochemistry and mass-transfer considerations

Imposing a strong centrifugal field enhances the electrochemical reaction rate by increasing the mass transfer rate at the electrodes. Studies on the hydrodynamics of multiphase flow with electrochemical reaction [8-9] are limited largely to mass transfer through a laminar boundary layer on a 2-dimensional flat surface. Multiphase electrochemically-reacting flow in porous media is not a well-researched area, especially when the influence of centrifugal fields is the main interest. Relatively few references exist describing the exploitation of intense centrifugal acceleration, these being mainly in chemical processing applications. Ramshaw's work [2] on 'process intensification' methods applied to industrial electrochemical reactors for chlorine production is perhaps the most relevant here.

Mass transfer in the case of single-phase flow of an electrolyte over a flat plate has been studied by many researchers, most notably Levich [8], whilst for conventional gas-diffusion electrodes various mechanistic models exist [20]. In all cases, the diffusion of a reactant *M* from the bulk (say M_b^{n+}) to the electrolyte-electrode interface (M_e^{n+}) is the rate-determining step, represented by $M_b^{n+} \rightarrow M_e^{n+}$. The diffusion process itself, in steady-state, is then governed by Fick's law of diffusion. This relates the flux, *Q*, of the reacting species across unit area to the concentration gradient and a local diffusion coefficient, *D*, which in the one-dimensional case is simply $Q = -D\dfrac{dc}{dx}$.

If the current-density (A/m^2) at which this reaction takes place is *i*, then

$$\frac{i}{nF} = -D\left(\frac{dc}{dx}\right)_{x=0}.$$

The rate at which M^{n+} diffuses to the electrode is equal to the rate at which it is consumed at the electrode. Therefore when the concentration varies linearly from the bulk value, c_b, to its concentration at the electrode, c_e, as in an unstirred solution, the concentration gradient is simply

$$\left(\frac{dc}{dx}\right)_{x=0} = \frac{c_b - c_e}{\delta}$$

where δ is the (constant) diffusion layer thickness. The diffusion current density in this case is

$$i = DnF\,\frac{c_b - c_e}{\delta}.$$

In the limit, as the current density is increased, the concentration gradient reaches a limiting value corresponding to $c_e = 0$, and the limiting current density i_L is then given by

$$i_L = \frac{DnFc_b}{\delta}.$$

This emphasizes the need to minimize the diffusion layer thickness δ in order to maximize the limiting current density. The ratio of current density to its limiting value is then

$$\frac{i}{i_L} = \frac{c_b - c_e}{c_b} = 1 - \frac{c_e}{c_b}$$

When mass transfer occurs by both diffusion and convection, the total current density in the steady state is given by the contributions from both effects, i.e. $i = i_D + i_C$ where i_D and i_C are respectively the current density fluxes for diffusion and convection normal to the electrode surface. The convection current i_C is often further expressed in terms of a transport number t^+ of the M^{n+} ion, i.e. $i_C = t^+ i$. Therefore

$$i = i_D + t^+ i = \frac{i_D}{1 - t^+}$$

and the total current density becomes

$$i = \frac{DnF}{1 - t^+}\,\frac{c_0 - c_e}{\delta}$$

where $0 \le t^+ \le 1$, δ is the constant diffusion layer thickness and c_0 is the bulk concentration of the M^{n+} ions. The current density i under conditions of diffusion and convection is therefore always greater than under diffusion alone.

Studies by Levich and others on reaction-driven diffusional flow, under natural convection, to a vertical plate are relevant to the centrifugal fuel cell in as far as the diffusion layer thickness varies with distance *x* from the leading edge of the plate. In the case of the air-electrode, this is the outer active radius of the disk electrode, $x = R_o - r$. Chemical reactions set up concentration gradients in the solution close to the electrode surface, and further density changes may also occur from exothermic heat release. Fluid motion is then due primarily to concentration differences across the thin diffusion layer. Levich estimated the diffusional flux under constant (1-g_o) acceleration, for natural convection conditions, to be of the form

$$i = D\left(\frac{\partial c}{\partial y}\right)_{y=0} = 0.7D\,Pr^{1/4}\left(\frac{g\alpha}{4\nu^2}\right)^{1/4}\frac{c_0}{x^{1/4}} = 0.7D\,Pr^{1/4}\left(\frac{gc_0}{4\nu^2\rho}\left(\frac{\partial \rho}{\partial c}\right)_{c=c_0}\right)^{1/4}\frac{c_0}{x^{1/4}}$$

When the concentration is expressed in grams per cm^3, then $\alpha = \dfrac{c_0}{\rho(c_0)}\left(\dfrac{\partial \rho}{\partial c}\right)_{c=c_0} \approx 1$ and the diffusional flux in natural convection can be assumed to be

$$i \approx 0.7 D\, Pr^{1/4} \left(\frac{g}{4\nu^2} \right)^{1/4} \frac{c_0}{x^{1/4}}.$$

The effective diffusion boundary layer thickness (omitting the c_0 term) is then given by

$$\delta \approx \frac{x^{1/4}}{0.7\, Pr^{1/4} \left(\frac{g}{4\nu^2} \right)^{1/4}}$$

Assuming typical values, e.g. plate height of 10 cm, Prandtl number Pr = 10, and gravitational constant g_0 = 10 m/s^2, ν = 10^{-6} m^2/s, the diffusion layer thickness is then about 0.035 cm. For a Pr = 100, δ is about 0.02 cm. Typical diffusion boundary layer thicknesses under natural convection are therefore greater than under forced convection, and thus the diffusional fluxes are correspondingly lower.

Under centrifuged conditions, the cell operates under spin-enhanced natural convection with 'artificial gravity' acting as the dominant radial-outward body-force in addition to normal gravity acting vertically down. In the centrifuged case (for $\omega^2 r >> g_o$), the standard acceleration due to gravity can be replaced by the centrifugal acceleration and the local diffusion layer thickness is

$$\delta = \frac{x^{1/4}}{0.7\, Pr^{1/4} \left(\frac{\omega^2 r}{4\nu^2} \right)^{1/4}}$$

which results in a reduced boundary layer thickness. Writing the local centrifugal acceleration in terms of an *acceleration enhancement factor* E_c, i.e.

$$g^* = \omega^2 R = E_c g_0$$

where g_0 is the standard acceleration due to gravity (9.8 m/s^2), the ratio of the diffusion layer thickness δ^* resulting from centrifugal acceleration, g^*, to the thickness δ_0 under normal 1-g_0 gravity, is

$$\frac{\delta^*}{\delta_0} = \left(\frac{g_0}{g^*} \right)^{1/4} = \frac{1}{E_c^{1/4}}$$

If the centrifugal field is equivalent to a constant acceleration enhancement factor E_c = 100, g^* = 100 g_0 ≈1000 m/s^2 over the whole area of the disk electrode, the thickness of the diffusion layer is reduced to $\delta^* = 1/100^{1/4} = 1/3.16 = 0.316$ or about 0.01 cm, i.e. roughly one third of the 1-g_o value.

Then, with a total current density given previously by

$$i \equiv i^* = \frac{DnF}{1-t^+} \frac{c_0 - c_e}{\delta^*},$$

the current density in the electrode when subjected to a higher constant acceleration g^* is increased from i to i^*, because of the reduction in diffusion layer thickness, in the ratio

$$\frac{i^*}{i} = \frac{\delta}{\delta^*} = \left(\frac{g^*}{g_0} \right)^{1/4} = E_c^{1/4} \quad \text{or} \quad \frac{i^*}{i} = \left(\frac{\omega^*}{\omega} \right)^{1/2} = \left(\frac{N^*}{N} \right)^{1/2}$$

where ω^* is the spin speed in radians/sec and N^* in revolutions/min. An increase in the local

limiting current density is therefore expected over that for natural gravity-driven convection, in proportion to the fourth root of the 'acceleration enhancement factor' or the square root of the speed ratio.

Some evidence that this simple relationship holds is indicated in Fig. 8, which presents results from an actual experiment. Of most interest is the plot of measured current against rotation speed for the final stable current achievable in the experiments, obtained at different speeds. Also indicated is the calculated current expected on the basis of the above-derived relation, referred to the first (lowest speed) reference current. The variation of hydrostatic pressure with speed is also shown. At higher rotation speeds, the increase in partial pressure of oxygen in the air could also influence the observed increase in current but this alone cannot explain the experimental results. The most significant effect is thought to be the reduction in boundary layer thickness at the electrode surface, as a result of the increase in 'artificial gravity', and the positive benefit this has on increasing the mass transfer rate.

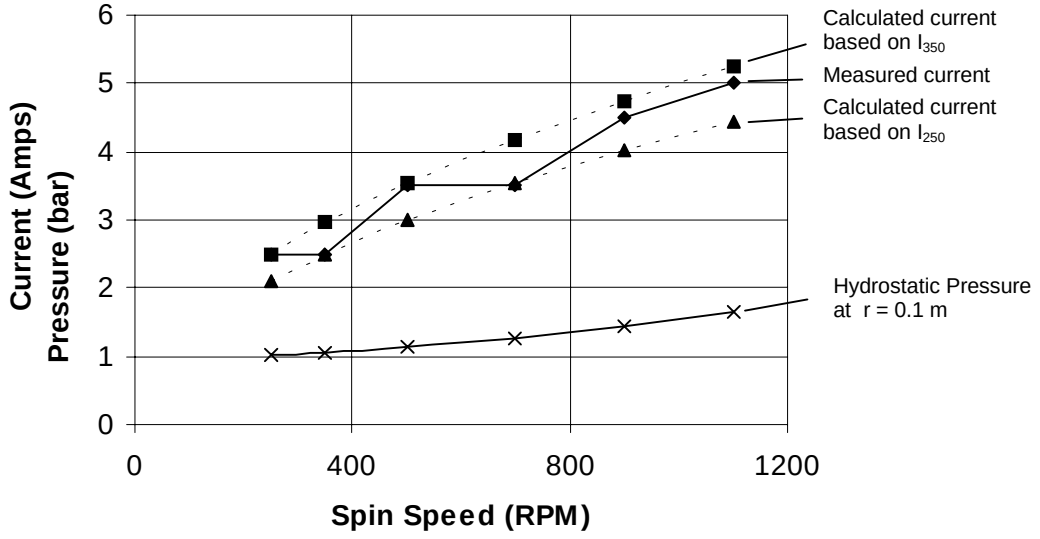

Figure 8. Variation of current against rotational spin-speed in an experimental centrifugal test rig.

In the centrifugal fuel cell, the local current flux density i^* must be averaged over the active geometric area of the disk-electrode between two (outer and inner) radii R_o and R_i, i.e.

$$I^*_{total} = \int_{R_o}^{R_i} i^* 2\pi\, r dr = \int_{R_o}^{R_i} \frac{DnF}{1-t^+} \frac{(c_0 - c_e)}{x^{1/4}} 0.7\, Pr^{1/4} \left(\frac{\omega^2 r}{4\nu^2} \right)^{1/4} 2\pi\, r dr\,.$$

With further simplifications, a comparison can be made of the 'centrifugal enhancement factor' with that of a reference 'static' disk-electrode over which a constant 1-g_0 radial acceleration is assumed to act, to compare the 'enhanced natural convection' with 'normal natural convection' on a circular disk. Taking the (normalized) outer radius R_o to be 1, and the outer and inner limits of integration to be arbitrarily 0.999 and 0.001, then with ω = 100 rad/s (equivalent to 1000 m/s^2), and with g_0 = 10 m/s^2, keeping all other parameters (labeled B) constant, numerical integration yields

$$\frac{I^*_{Centrif.}}{I_{Static}} = \frac{\int_{R_o}^{R_i} B\,\omega^{1/2} \left(\frac{r}{(1-r)} \right)^{1/4} r\, dr}{\int_{R_o}^{R_i} B\, g_0^{1/4} \left(\frac{1}{1-r} \right)^{1/4} r\, dr} = \frac{B\,\omega^{1/2} \int_{0.001}^{0.999} \left(\frac{r^5}{1-r} \right)^{1/4} dr}{B\, g_0^{1/4} \int_{0.001}^{0.999} \left(\frac{r^4}{1-r} \right)^{1/4} dr} \cong 0.911 \frac{100^{1/2}}{10^{1/4}} = 5.124$$

Thus a typical increase in total current density of about 5 might be expected with an imposed centrifugal field (at the outer radius) of a magnitude 100 times the standard gravitational acceleration g_0. This increase is due only to the reduction in diffusion layer thickness. Additional benefits should also derive from the increase in the partial pressure of the gas phase arising from the increased hydrostatic head in the cell. By extension, an acceleration of say 1000-*g* (with ω = 1000 rad/s) might be expected to yield an increase in current density of 16.2, which is a very worthwhile improvement.

3. EXPERIMENTS WITH A PROTOTYPE CENTRIFUGAL ZINC-AIR CELL

A small prototype centrifugal zinc-air battery has been constructed (see Acknowledgements) and has undergone a first series of tests. Based on the cross-section shown in Fig. 5, this device utilizes two porous disk-shaped zinc anodes and two carbon air-electrodes, in a KOH aqueous electrolyte of concentration 6-8 *M*. It can spin at speeds up to 1200 rpm, and at a nominal maximum speed of 1000 rpm develops 100-*g* (~1000 m/s^2) acceleration at the outer radius of the air electrode (r = ~ 0.1 m).

First test results have indicated a clear increase in current (Fig. 8) and voltage (Fig. 9). This increase in voltage might be attributable to the increase in partial pressure of the oxygen in the air. The measured polarization curve (Fig. 10) shows the cell's operating voltage/current characteristics for speeds from 250 rpm up to 1100 rpm. This indicates that the obtained current falls from the initial open circuit voltage (E_0) of about 1.38 V to its operating voltage as higher currents are drawn from the cell, as characterized by the classical polarization curve shown previously in Fig. 1.

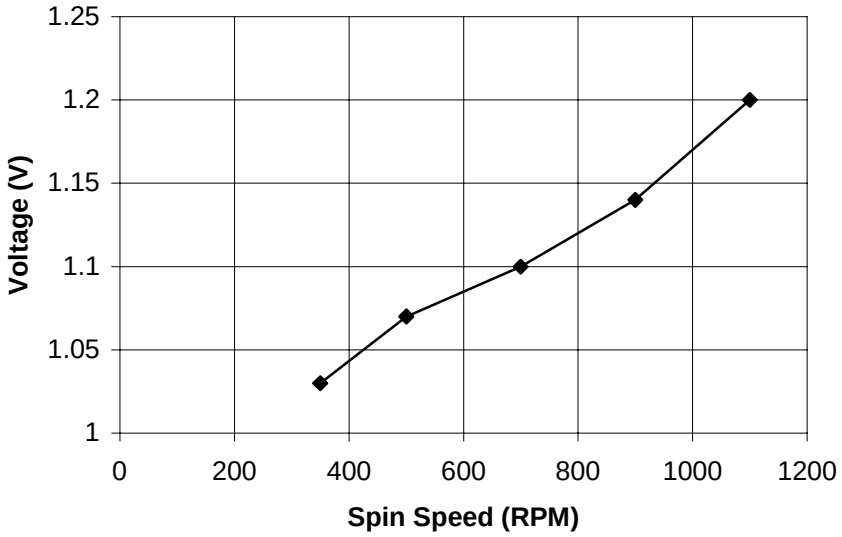

Figure 9. Variation of voltage with rotational spin speed in prototype centrifugal cell (constant current, I = 3.5 A).

As indicated in Fig. 10, as the speed increases the point at which voltage instability occurs shifts towards higher currents and higher sustained voltages. At the highest speed used in the tests, the voltage is maintained above 1.15 V until a current of about 5 V is reached, when voltage breakdown occurs. Thus a clear indication of increasing voltage and current (power) accompanies the increase in spin speed. Porous electrodes are used to reduce the local current density by providing a large surface area within a given geometric dimension of electrode. For a given operating current, the activation or charge-transfer polarization at the electrode active surface is in this way reduced. The concentration polarization results from mass transfer rate limitation in the boundary layer

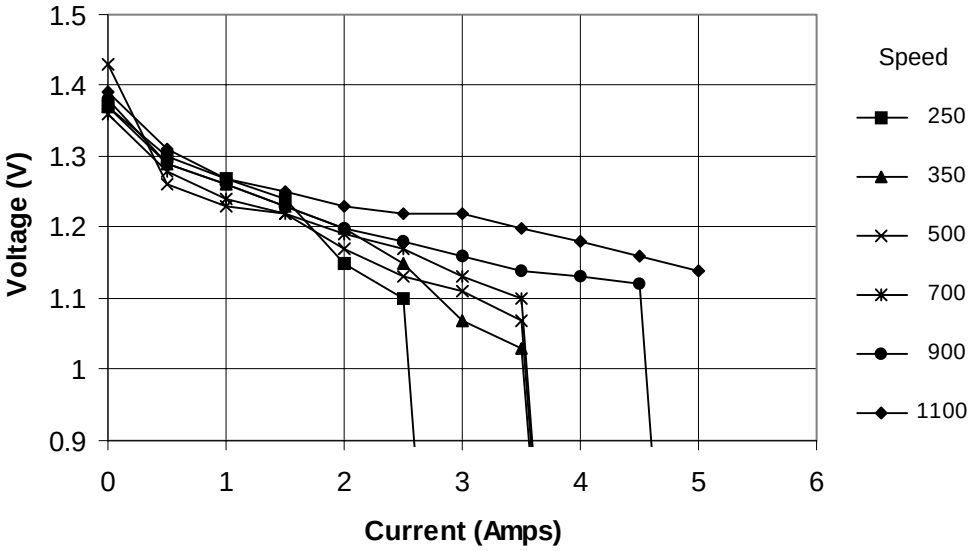

Figure 10. Polarization curve obtained for prototype centrifugal cell at different spin speeds

adjacent to the electrode surface. By providing a good flow of electrolyte past the electrodes ensures that products from the electrochemical reaction are diffused and transported away from the electrode surface, increasing the local concentration gradient and minimizing the concentration boundary layer thickness. In the centrifugal cell, most probably it is this latter effect which has most benefit in improving the cell's polarization curve.

Further experiments are planned in the near future with a novel design of 'ribbed' electrode and also with various porous reticulated metal-foam 3-dimensional electrodes. The ribbed electrodes are specially made compressed carbon disk electrodes, fabricated in such a way as to form multiple radial walls (ribs) raised above the flat surface of the disk by about 1 mm. When 'sandwiched' between other components, these ribs form radial convergent channels through which air can flow from the outer radius (i.e. the sparger) to the inner radius of the disk and the electrolyte free surface. This design provides a higher surface area for reaction and lends itself to a more compact design of electrode stack. Further experiments with reticulated metal foam electrodes, planned in the near future, will be the first attempts to utilize 3-dimensional disk- or torus-shaped air-electrodes in which both air and KOH flow inside the electrode matrix.

4. CONCLUSIONS

Some conclusions based on recent developmental experiences and the first tests of a prototype centrifugal electrochemical cell are as follows:

(1) A small centrifugal zinc-air cell has been successfully constructed, having two pairs of flat disk electrodes in a potassium hydroxide electrolyte, capable of rotation speeds up to 1200 rpm and centrifugal accelerations of about 130-*g* at the outer radius of the electrodes.

(2) Intense centrifugal fields can be used to advantage to increase mass transfer rates and to improve the electrochemical reaction process in batteries and fuel cells. With careful design, the energy needed to maintain rotation can be kept arbitrarily small.

(3) Initial tests demonstrate that the centrifugal cell develops monotonically increasing current and voltage characteristics with increasing spin speeds. The 'acceleration enhancement factor' has a positive effect on the electrochemical oxidation and reduction processes occurring at the electrodes and this is believed to be a strong

factor in reducing the concentration over-voltage.

(4) The major beneficial effect is thought to be due to the increased mass transfer rate attributable to the reduction in concentration boundary layer thickness at high centrifugal accelerations, and the consequential reduction in concentration polarization which results.

(5) Preliminary analysis of the results suggests that the observed increase in current can be correlated roughly to the 4^{th} root of the ratio of centrifugal accelerations pertaining to any two spin-speeds, or to the square root of the spin-speed ratio. These ratios determine the relative thickness of the boundary layer at different rotation speeds and hence the mass transfer rates.

(6) A semi-theoretical approach to exploiting intense centrifugal fields has been presented by way of optimizing the hydrodynamic flow conditions to achieve high mass-transfer rates and to increase the threshold for voltage breakdown caused by molecular diffusion limitations.

(7) Further experiments are planned with various new types of porous electrodes with the aim of improving the performance and design of electrochemical energy generation/storage devices.

ACKNOWLEDGEMENTS

This work was funded by the European Commission in the framework of the 'JRC Innovation Project Competition 2000'. The overall design, development and testing of the centrifugal cell was carried out under contract by ZOXY Energy Systems AG, Oberderdingen-Flehingen, Germany. Fabrication and testing of the air-electrodes was made in collaboration with the Central Laboratory for Electrochemical Power Sources of the Bulgarian Academy of Sciences, Sofia. The effort of both teams is hereby gratefully acknowledged.

REFERENCES

1. A. B. Hart and G. J. Womack, *Fuel Cells - Theory and Application*, Chapman and Hall, 1967.
2. C. Ramshaw, *The opportunities for exploiting centrifugal fields*, Heat Recovery Systems and CHP, vol. 13, No. 6, pp.493-513, 1993.
3. C. Ramshaw, *"HiGee" Distillation - An example of Process Intensification*, The Chemical Engineer, Feb. 1983.
4. B. Worth, European patent application No. 98308577.0, (pending) October 1998.
5. J. P. Collman, M. Marrocco, P. Denisevich, C. Koval, F.C. Anson, *Potent catalysis of the electroreduction of oxygen to water by dicobalt porphyrin dimers adsorbed on graphite electrodes,* J. Electroanal. Chem., 101 (1979), pp. 117-122, Elsevier Sequoia, NL, 1979.
6. E. Yeager, *Electrocatalysts for O_2 reduction*, Electrochimica Acta, Vol.29, No. 11, pp. 1527-1537, 1984, Pergamon Press Ltd, UK, 1984
7. I. Iliev, *Air electrodes for aluminium-air batteries*, Bulletin de la Societe Chimique Beograd 48 (Supplement) S 317 - S 338 (1983), Contributed paper at the Second International Workshop on Reactive Metal-Air Batteries (Belgrade), Sept. 3-4, 1982, Belgrade, Yugoslavia.
8. V. G. Levich, *Physicochemical Hydrodynamics,* Prentice-Hall, Inc., 1962.
9. J. O'M. Bockris and S. Srinivasan, *Fuel Cells: Their Electrochemistry,* McGraw-Hill Book Company, 1969.

10. L. J. M. J. Blomen and M. N. Mugerwa, *Fuel Cell Systems*, Plenum Press, Ch. 1, 1993.
11. K. Kordesch, and G. Simader, *Fuel Cells and Their Applications*, VCH Publishers, 1996.
12. D. A. J. Rand, R. Woods and R. M. Dell, *Batteries for Electric Vehicles*, Research Studies Press, John Wiley & Sons Inc, 1997.
13. D. Linden, *Handbook of Batteries*, McGraw-Hill, Inc., 1995.
14. B. Worth, *The Centrifugal Metal-Air Fuel Cell concept - Prospects for future vehicle propulsion*, Institution of Mechanical Engineers' Conference Transactions, 1999 C575/021.
15. J. Bear, *Dynamics of Fluids in Porous Media*, Dover Publications Inc., 1988.
16. G. K. Batchelor, *An introduction to Fluid Dynamics*, Cambridge University Press, 1994.
17. S. L. Soo, *Particulates and Continuum Multiphase Fluid Dynamics*, Hemisphere Publishing Corp., 1989.
18. D. Butterworth, and G. F Hewitt (editors), Two-phase Flow and Heat Transfer, UKAEA Research Group, Harwell series, Oxford University Press, 1978.
19. V. Balasundarum, J. E. Porter, and C. Ramshaw, *Process intensification: A Rotary Seawater Deaerator*, Separation of Gases, 5th Proc. B.O.C. Priestley Conference, Birmingham, 1990 Royal Society of Chemistry, Cambridge, pp. 306-328.
20. D. T. Wasan, T. Schmidt, and B. S. Baker, *Mass transfer in fuel cells: Part 1. Models for porous electrodes*; Chemical Engineering Progress Symposium Series, 1967, No. 77, Vol. 63.